# A Guided Tour to Wonderland: Visualizing the Slow-Fast Dynamics of an Analytical Dynamical System

Rainer Wegenkittl, Eduard Gröller, Werner Purgathofer

Institute of Computer Graphics
Technical University of Vienna

**Note to the reviewers**: Please use `http://www.cg.tuwien.ac.at/~rainer/vis96/` to see the animation sequences and also the color plates

***Abstract:*** *The analysis of complex dynamical systems produces large amounts of data that have to be interpreted efficiently. Visualizing the phase space of such systems illustrates geometrically the behavior of the underlying dynamics. This work investigates the visualization of Wonderland, a four dimensional econometric model, which describes interactions between population growth, economic activity and environmental implications. Wonderland belongs to a class of interesting dynamical systems with a pronounced slow-fast dynamics, i.e., some variables are changing much faster than others. Furthermore the behavior of the Wonderland model is characterized by manifolds which are not streamsurfaces, i.e., the flow does not stay within these surfaces. This paper discusses the application and adaptation of various visualization techniques to analytical dynamical systems with special properties as mentioned above.*

**Keywords:** vector field visualization, complex dynamical systems

## 1. Introduction

Scientists in various fields, e.g., chemistry, physics, biology, economy, medical research, and fluid dynamics, investigate *dynamical systems*. Any set of variables whose configuration describe the state of a mathematical model is thereby called dynamical system, if its evolution in time is determined by a set of rules [Tson92]. To formalize these rules many natural phenomena are approximately described by differential or difference equations. The rules specifying the evolution of a continuous dynamical system (also called *flow*) are given as a set of differential equations. An important characteristic of a dynamical system is whether it is time-dependent or not. Analyzing time-dependent models is much more complicated than analyzing time-invariant systems.

The dimension of a dynamical system depends on the number of variables which completely describe its state. If each of these variables (degrees of freedom) is assigned to a coordinate axis, the behavior of the system is investigated in the so-called *phase space*. One point in phase space corresponds to a specific state of the system at one moment in time. The temporal evolution is given as a one-dimensional curve (*trajectory*) in phase space. Since realistic models typically consist of many state variables, the dimension of a dynamical system can be rather high. Obviously the direct visualization of systems with a dimension larger than three is a non-trivial problem. Thus the dimension of the system has to be reduced by, for example, projecting the system onto a lower dimensional cross section.

The presented work concentrates on the visualization of a four dimensional continuous dynamical system (Wonderland model) coming from the field of econometrics. This system has some features which make its analysis a very interesting challenge. Its temporal evolution, for example, is characterized by a so-called *slow-fast* dynamics. This means, that some of the system variables vary much faster than others. The difference in velocity is on the order of one or even two magnitudes and thus poses difficulties for the visualization process.

It turned out that certain 2D *manifolds* play an essential role in the analysis of the Wonderland model. The specific manifolds under consideration are surfaces, on which the derivative of a system variable is equal to zero. Due to their definition, these manifolds do not describe streamsurfaces, which means, that they are intersected and crossed by the systems flow. Thus visualization techniques which are specifically designed for streamsurfaces and which are based on the assumption that a flow starting on the surface will stay within the surface cannot be used for the above mentioned manifolds.

Our cooperation with researches in econometrics where stimulated by the fact that in this research area typically only simple visualization techniques have been used so far. Examples for this approach are still images, simple line drawings, 2D projections or cross-sections of higher-dimensional phase spaces, and scarce use of color.
Therefore this paper discusses various advanced visualization techniques and adaptations thereof to enable a graphical exploration of analytically defined systems as given in econometrics. The adapted techniques are then applied to analyze a specific model, i.e., the *Wonderland* model. The aim of the work is to increase an intuitive understanding of the complicated dynamics of slow-fast systems. It is intended to offer scientists, which have not used the full potential of advanced visualization techniques so far, additional and efficient tools in their research work.

## 2. Wonderland, the Model

### 2.1 Model Definition

The world we shall step into now is a continuous version of W. C. Sanderson's *Wonderland* model [Sand94] of economic, demographic and environmental interactions, that has been studied in [MiPr95] and [GrWe95]. The dynamics in Wonderland is determined by four state variables:

- *x(t)*... population
- *y(t)*... per capita output (economic performance)
- *z(t)*... quality of environment (natural capital)
- *p(t)*... pollution per unit of output

which evolve according to the following set of differential equations

$$\begin{aligned}
\frac{dx}{dt} &= x \cdot n(y,z) \\
\frac{dy}{dt} &= y \cdot \left[\gamma - (\gamma+\eta)(1-z)^{\lambda}\right] \\
\frac{dz}{dt} &= \nu \cdot z \cdot (1-z)\left[-\frac{\omega \cdot f(x,y,z,p) - \delta \cdot z^{\rho}}{\omega \cdot f(x,y,z,p) - \delta \cdot z^{\rho} + 1}\right] \\
\frac{dp}{dt} &= -\chi \cdot p
\end{aligned} \tag{1}$$

where the population growth rate is given by

$$n(y,z) = b(y,z) - d(y,z),$$

which is the difference of the crude birth rate

$$b(y,z) = \beta_1\left[\beta_2 - \frac{1}{2}\left(1 + \frac{\beta \cdot \bar{y}(y,z)}{\beta \cdot \bar{y}(y,z) + 1}\right)\right]$$

and the crude death rate given by

$$d(y,z) = \delta_1\left[\delta_2 - \frac{1}{2}\left(1 + \frac{\alpha \cdot \bar{y}(y,z)}{\alpha \cdot \bar{y}(y,z) + 1}\right)\right] \cdot \left(1 + \delta_3 (1-z)^{\vartheta}\right)$$

$\bar{y}(y,z) = y - c(y,z)$ indicates the net per capita output with $c(y,z) = \varphi \cdot (1-z)^{\mu} \cdot y$ giving the pollution control. The pollution flow, which refers to the introduction of new pollutants into the environment, is given by

$$f(x,y,z,p) = p \cdot x \cdot y - \frac{\kappa}{2}\frac{\varepsilon \cdot c(y,z) \cdot x}{\varepsilon \cdot c(y,z) \cdot x + 1}.$$

The entire system contains twenty parameters but is still a very rough approximation of reality. The components of the system can be interpreted as follows. Natural capital *z* is assumed to vary in the interval [0,1]. If the environment is not polluted at all natural capital z is equal to one. On the other extreme, when the environment is so polluted that it produces the maximum possible damage to human health and to economy then *z* is equal to zero. The endogenous population growth rate *n(y,z)* is defined by the difference between the crude birth rate (relative number of births per unit of time) and the crude death rate (relative number of deaths per unit of time). Net per capita output $\bar{y}(y,z)$ is defined as the difference of per capita output and per capita expenditures on pollution control *c(y,z)*. Pollution control expenditures are assumed to depend on how polluted the environment is and not on the current flow of emissions. Pollution per unit of output *p* is assumed to fall exponentially towards zero due to improving technology and increasing consciousness regarding the environment.
Depending on a slight variation of various parameters adjacent trajectories evolve in a completely different way. According to this, three main scenarios can be distinguished, when starting with an almost non-polluted environment. In the *dream scenario* no rapid environmental changes occur, thus resulting in a clean environment with growing population and economy. In the *horror scenario* a sudden catastrophic environmental decline towards a totally polluted environment occurs. The environment never regenerates which leads to a collapse in population size and economy. In the *escape scenario* the system regenerates after a sudden environmental crash. Cycles of sudden and severe environmental degradation and regeneration occur repeatedly (Figure 1).

The above mentioned different scenarios (dream, horror and escape scenario) basically depend on the parameters $\chi$ (specifying the decrease of pollution per unit of output in successive time periods) and $\kappa$ (describing the effectiveness of pollution control). Starting with the dream scenario and taking a smaller $\chi$, which means a lower rate of decrease for the (exponentially falling) pollution per unit of output $p$, the system changes to the horror scenario. Now when the parameter $\kappa$ is increased, which means a more effective pollution control, the collapse of the environment can be stopped and the system behaves according to the escape scenario.
In Figure 1 the three scenarios are shown in phase space. All three trajectories start at $x$=$y$=$p$=1, and $z$=98. The orbit of the dream scenario stays always near $z$=1, $x$ and $y$ increase and $p$ decreases forever, whereas in the horror scenario and the escape scenario the variable $z$ suddenly decreases rapidly. In the horror scenario $z$ decreases down to its lowest value $z$=0, while in the escape scenario the environment regenerates and $z$ increases again, first slowly then fast, until $z$ is again close to its highest possible value. For more details see [MiPr95], [GrWe95].

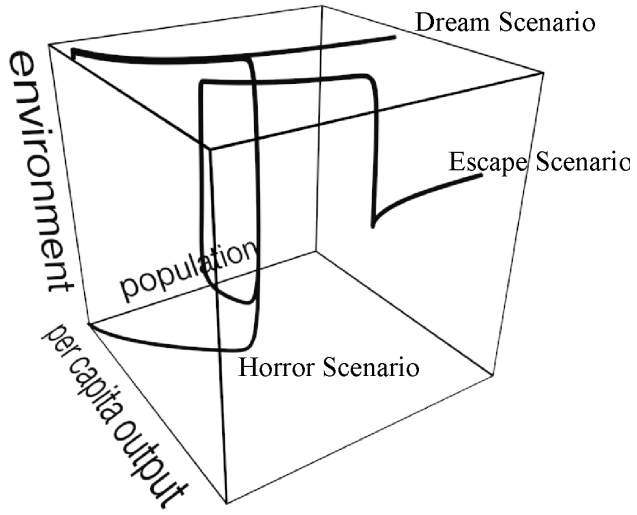


Figure 1: The dream, horror and escape scenario shown in phase space

### 2.2 Slow-Fast Dynamics

The set of differential equations of the Wonderland model shows a slow-fast behavior, which means, that one of the systems variables, i.e., $z$, varies much faster than the others, i.e., $x$, $y$, and $p$. For the analysis of this phenomena the system can be rewritten using a scaling factor $\varepsilon$ with $0 < \varepsilon << 1$. In the context of singular perturbation theory $\varepsilon$ is called the perturbation parameter. The analysis of the system is basically done by separating the system into its slow and fast components which are both analyzed by themselves. The *reduced system* which captures the slow dynamics is given as

$$\frac{dx}{d\tau} = x \cdot n(y,z)$$

$$\frac{dy}{d\tau} = y \cdot \left[\gamma - (\gamma + \eta)(1-z)^{\lambda}\right]$$

$$0 = \nu \cdot z \cdot (1-z)\left[-\frac{\omega \cdot f(x,y,z,p) - \delta \cdot z^{\rho}}{\omega \cdot f(x,y,z,p) - \delta \cdot z^{\rho} + 1}\right]$$

$$\frac{dp}{d\tau} = -\chi \cdot p$$

where $\tau$ indicates the rescaled time ($\tau = \varepsilon \cdot t$). The *layer* system captures the fast dynamics and is given as

$$\frac{dx}{dt} = 0$$

$$\frac{dy}{dt} = 0$$

$$\frac{dz}{dt} = \nu \cdot z \cdot (1-z)\left[-\frac{\omega \cdot f(x,y,z,p) - \delta \cdot z^{\rho}}{\omega \cdot f(x,y,z,p) - \delta \cdot z^{\rho} + 1}\right]$$

$$\frac{dp}{dt} = 0$$

Both systems approximate certain aspects of the dynamics of the original model but with limited validity in phase space and time. However, one may arrive at a global picture of the dynamics by matching the solutions of these two systems accordingly. This can be done with techniques of (geometric) singular perturbation theory. For details see [MiRo80], [Jone95], [Feni79]. With analyzing and visualizing equilibrium manifolds (described in the following section) of the reduced system we gain qualitative information on the original Wonderland system.

### 2.3 Equilibrium Manifolds

The qualitative behavior of the Wonderland model can be analyzed by investigating the reduced and the layer system. The areas of phase space where the reduced system is given is of special interest and will be visualized in subsequent sections. These regions are specified by the following equation (see the defining equations of the reduced system):

$$0 = \nu \cdot z \cdot (1-z) \cdot \left[ -\frac{\omega \cdot f(x,y,z,p) - \delta \cdot z^{\rho}}{\omega \cdot f(x,y,z,p) - \delta \cdot z^{\rho} + 1} \right]$$

The regions defined by the above equation are two-dimensional surfaces which are called *equilibrium manifolds*. The flow at a point of an equilibrium manifold is parallel to the *xy*-plane which means that the environment is stable or in equilibrium at such positions. The above equation holds if one of the following conditions are fulfilled:

- $z = 0$
- $z = 1$
- $\omega \cdot f(x,y,z,p) - \delta \cdot z^{\rho} = 0$

Each of these three cases produces a separate two-dimensional manifold. In the first case ($z = 0$) the equilibrium manifold corresponds to the *xy*-plane and is denoted by $Z_0$. If the state of the system is in $Z_0$ the environment is totally destroyed and cannot regenerate anymore. The second case ($z = 1$) specifies a manifold called $Z_1$ which corresponds to a plane parallel to the *xy*-plane at $z = 1$. The environment is in perfect condition in this case. The third and most interesting manifold, called $Z_c$, is described by a curved surface. Its shape and position decisively depend on parameters $\kappa$ and $\chi$ and varies with changing pollution per unit of output *p*. The rate of this change determines if in a specific situation with fixed parameter values either the dream, horror or escape scenario will evolve.

# 3. Visualization Techniques for the Slow-Fast Dynamics of the Wonderland Model

Visualizing the behavior of dynamical systems is crucial for a deeper understanding of the underlying dynamics. Different techniques are already known in the field of fluid dynamics to visualize 2D and 3D vector fields [Hans93], [PoWa93], [PoWi94]. The visualization of a dynamical system can be done by displaying either global or local properties of the system. Flow topology information is well suited to allow an analysis of the global behavior of a dynamical system. The analysis process consists of the identification and the characterization of special subsets of the dynamical system, e.g., equilibrium manifolds in the case of the Wonderland model.
Surface oriented visualization techniques for dynamical systems are usually tailored to streamsurfaces. A streamsurface is generated by following a set of initial states which are positioned on a curve through phase space. A streamsurface cannot be crossed by any other trajectory of the system and the flow starting on a streamsurface remains inside the surface itself. Several techniques, e.g., spot noise [Wijk91] and line integral convolution [CaLe93], are well suited to visualize the flow on a streamsurface but it is not straightforward to apply these approaches to surfaces which are crossed by the flow of the system like the equilibrium manifolds of the Wonderland model. In the following sections we will discuss this issue. In the context of an equilibrium manifold we had to concentrate on the flow *close* to the manifold instead of on the flow *within* it. Visualizing the largely varying flow velocity in a system with slow-fast dynamics poses another problem. Nonlinear scaling and animated textures where taken to solve this task.

## 3.1 Velocity Visualization with Animated Textures

Trajectories in a dynamical system are represented by three-dimensional geometric objects called *tubes*. A tube is generated by extruding a circle along the path defined by an evolving trajectory. This approach allows correct shading of the trajectory, which facilitates to recognize the spatial arrangements of objects in phase space. A trajectory is thus given as a regular cylindrical mesh of quadrilaterals whose vertices can be assigned various visual properties, e.g., color, opacity, texture.
One can think of several possibilities to encode velocity along a trajectory. Color coding the velocity gives only a qualitative distinction between high-velocity and low-velocity regions of a trajectory. Another approach varies the thickness of the tube according to velocity, i.e., the tube is thick in low-velocity regions and thinner where the velocity is higher. To avoid cluttered phase space displays the diameter of a tube is rather small which implies that only a limited number of distinct velocities can be encoded with this approach. Animating the temporal evolution of a trajectory gives a clear feeling of the flow velocity. But single images show only the state of the trajectory at one specific point in time without any hints on the velocity. Therefore we were looking for a technique which is suitable to illustrate velocity not only in an animation sequence but at the same time in single images as well. One approach is to display the entire trajectory and position geometric objects, e.g., spheres, at temporally equidistant locations along the trajectory. This, however, increases the geometric complexity of the phase space representation and might hamper the ease of interpretation. We therefore used special types of textures to map a spiral structure onto the

tube representation of trajectories. The distance between adjacent coils of the spiral encodes flow velocity. In high-velocity regions the distance between adjacent coils is large whereas in low-velocity regions adjacent coils are close together (see color plates). We used a texture as given in Figure 2 which is wrapped around the trajectory along the u-coordinate of the texture coordinate system. The texture itself is periodic both in u- and v-direction. Periodicity along the u-coordinate ensures continuity at the seam of the wrapped texture. Periodicity along the v-direction ensures continuity along the flow when covering the trajectory with copies of the texture image. The texture is stretched or compressed along the v-direction according to the locally varying velocity. This produces the effect of a spiral with unevenly spaced coils. Figure 3 illustrates a typical trajectory of the Wonderland model where temporally equidistant positions are marked. The distance between adjacent marks shows the local velocity. These temporally equidistant but spatially non-equidistant positions are mapped onto the v-coordinate of the texture. Thus in high-velocity regions the texture is stretched whereas in low-velocity regions it is compressed.

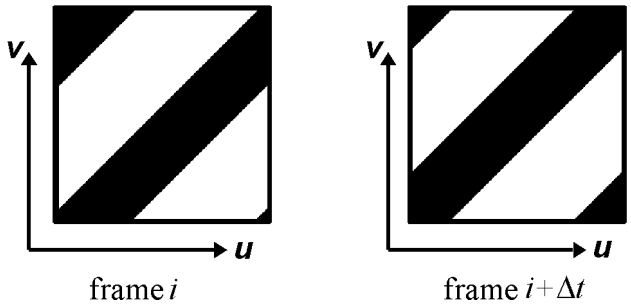


Figure 2: Two frames of an animated texture

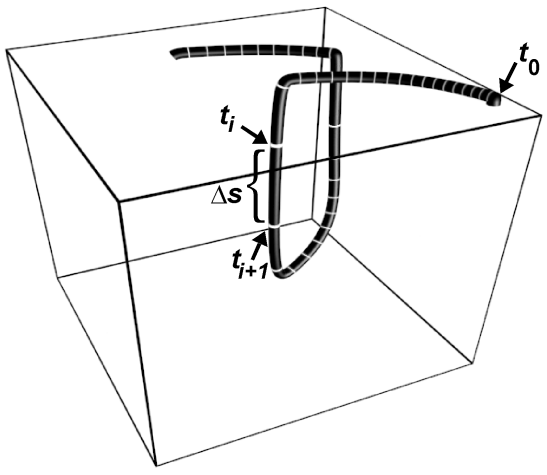


Figure 3: Trajectory with temporally equidistant marks

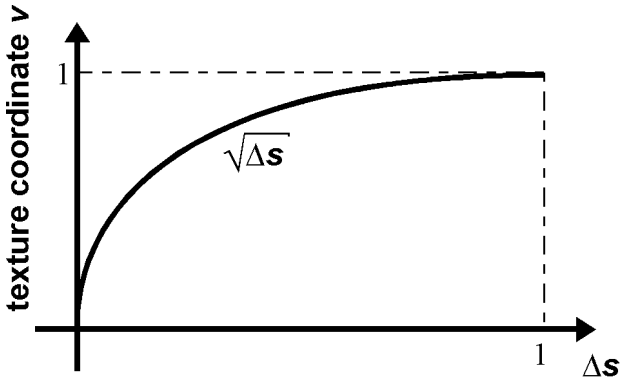


Figure 4: Nonlinear scaling of velocity values to adjust for the slow fast dynamics of the Wonderland model

Due to the slow-fast dynamics of the Wonderland model the velocity range is about two orders of magnitude, i.e., the largest velocity value is about 100 times larger than the smallest value. Furthermore most of the time the velocity is either very small or very large. To handle this large velocity variation a nonlinear dampening is done according to the function given in Figure 4. $\Delta s$ corresponds to the length of the trajectory between adjacent temporal positions (see also Figure 3). Applying the function of Figure 4 stretches the texture in regions of slow velocity and therefore avoids spirals with indistinguishably close coils. In the interpretation phase the user, however, has to be aware of this nonlinear transformation.

Using the texture as described above produces still images of the entire trajectory where the flow velocity is easily recognizable. When calculating animation sequences where the whole trajectory is present from the beginning it is necessary to convey to the viewer a sense of motion. We achieve such an effect by rotating the spiral texture on the trajectory which is realized by an animated texture. An animated texture is an animation sequence of texture maps. For each frame of the actual animation sequence the corresponding texture map of the animated texture is used. In our case the animated texture simply consists of periodically cycling the texture of Figure 2 in v-direction, i.e., consecutive maps of the animated texture differ by shifting the image upwards by one scanline and pasting the top scanline into the bottom scanline of the previous texture map. Figure 2 shows two texture maps of the animated texture (diagonal stripe moving horizontally through the image) which was used in the color plates and animation sequences. Animated textures proved to be very useful in illustrating flow motion along static representations of trajectories.

### *3.2 Visualizing Equilibrium Manifolds*

The equilibrium manifolds $Z_0$, $Z_1$, and $Z_c$ of section 2.3 are topological structures that decisively

characterize the behavior of the Wonderland model. The first two ($Z_0$, $Z_1$) are given as simple planes in phase space, the third one ($Z_c$) is given as a curved surface. The system behavior is not only determined by the position of the manifolds but also by their properties. Positions on a manifold can be *attracting* and *repelling*. If a specific region of a manifold is attracting all trajectories in the neighborhood of that region will approach the manifold over time. On the other hand a region of a manifold is called repelling, when every trajectory in the neighborhood of that region of the manifold is moving away over time. In our case an equilibrium manifold is either entirely attracting or repelling or it consists of two contiguous and connected regions, one attracting and one repelling. The property of a position on a manifold of being either attracting or repelling is determined by local linearization. If the system is given as $\dot{\vec{x}} = f(\vec{x})$ then the eigenvalues of the Jacobian $\nabla f(\vec{x})$determine the type of stability (e.g., attracting or repelling). In the case of the Wonderland model the layer system (fast dynamics) is taken to perform this analysis. Thus the Jacobian is simply the derivative of *dz/dt* (see section 2.2). A location on an equilibrium manifold is attracting (repelling) if the sign of the real part of this derivative is negative (positive). Furthermore $Z_0$ is attracting as long as $p$ is bigger than $\varphi \cdot \kappa / \varepsilon$. In this case a point of $Z_1$ is attracting if $x \cdot y$ is less than a certain threshold and is repelling when $x \cdot y$ is larger than this threshold.

As soon as the exponentially decreasing state variable $p$ falls below $\varphi \cdot \kappa / \varepsilon$, $Z_0$ becomes repelling near the origin and $Z_1$ behaves in the same way as before. $Z_0$ and $Z_1$ change their stability properties along critical curves called $C_0$ and $C_1$. These curves are exactly the intersection curves between $Z_0$, $Z_c$ (for $C_0$) and $Z_1$, $Z_c$ (for $C_1$) respectively.

With $p > \varphi \cdot \kappa / \varepsilon$ all of the manifold $Z_c$ is repelling, but when that condition does not hold anymore, $Z_c$ becomes folded. The upper branch of the fold is still repelling while the lower branch becomes attracting. The upper and lower part of the fold are separated by the critical curve $C_c$ (see color plates).

The qualitative behavior of the Wonderland model, i.e., appearance of the dream, horror or escape scenario can now be easily described by analyzing the equilibrium manifolds. If, for example, we start the numerical simulation with $x = y = p = 1$ and $z = 0.98$, than $Z_1$ attracts the resulting trajectory. In case condition $x \cdot y \cdot p < \delta / \omega$ always holds (depending on the chosen values of parameters $\kappa$ and $\chi$) the attracting property of $Z_1$ produces an almost perfect environment as described by the dream scenario (see Plate 1 and Plate 2). When the critical curve $C_1$ is, however, crossed by the trajectory during the evolution of the system, the trajectory is now close to the repelling part of $Z_1$ and therefore the environment has to decline. An interesting phenomenon occurs in this case. The trajectory does not decline immediately after it crosses $C_1$ but stays close to the repelling part of $Z_1$ for a while. This *time delay* is due to the fact that the trajectory has been converging exponentially to the attracting part of $Z_1$. Therefore it takes some time until the diverging influence of the now repelling part of $Z_1$ becomes visible and causes the trajectory to fall off rapidly (fast dynamics). This phenomenon has some uncomfortable interpretation: the environment and the system may already be in an unstable state beyond the point of no return although the state variables still indicate a clean and healthy environment.

If the trajectory crosses $C_1$ and the manifold $Z_c$ is not folded yet, the trajectory falls down towards the attracting part of $Z_0$. Since $x$ and $y$ are declining functions when $z$ is close to zero, the whole system has to collapse towards the origin. This constellation therefore produces the horror scenario (see Plate 3 and Plate 4). If contrary to the horror scenario the manifold $Z_c$ is already folded, the falling trajectory gets caught by the attracting lower branch of $Z_c$ crosses the manifold parallel to the xy-plane (see definition of $Z_c$) and is induced to move upwards again. As soon as the trajectory comes close to the upper part of $Z_c$ which is repelling it moves away from $Z_c$ and is again rapidly pulled to the attracting part of $Z_1$. The interpretation is that after a near-fatal crash the environment is able to regenerate resulting in the escape scenario (see Plate 5 and Plate 6).

Manifolds are represented as two dimensional regular quadrilateral grids. These mesh surfaces are easily shaded and textured, thus giving a better feeling of the shape of the manifolds. Due to the positions of the manifolds within phase space typically a large amount of occlusion occurs. This problem is solved by rendering the manifolds transparently. To distinguish attracting regions from repelling ones we use color coding. Attracting portions of the equilibrium manifolds are rendered in green, while repelling parts are displayed in red. This allows a quick and easy estimation of the flow within the system. Color coding in connection with transparency has, however, a disadvantage. For certain camera positions the colors of several overlapping manifolds are mixed and somewhat irritating colors are generated. This problem is avoided by rendering the simple manifolds $Z_0$ and

$Z_1$ not as surfaces. Instead they are represented by their corresponding border curves which are modeled as opaque tubes. The coloring of these tubes again reflects the stability of the enclosed region.
The geometric shape of transparent and curved surfaces like $Z_c$ is much better recognizable with texture mapping. As shown in most of the color plates a transparency texture is mapped onto $Z_c$. The transparency texture modulates the transparency of $Z_c$, i.e., some parts of $Z_c$ are more transparent than others.

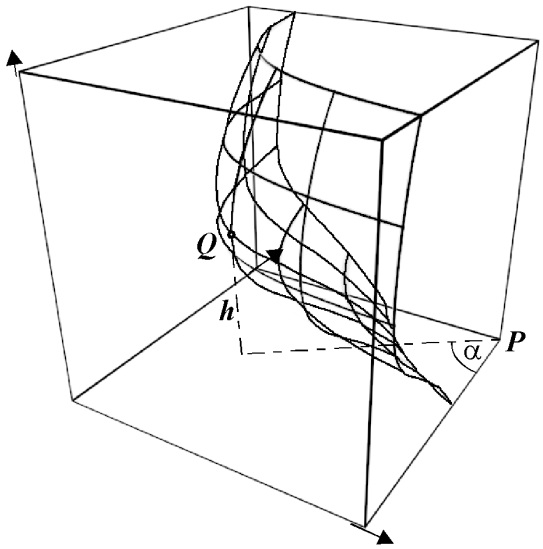


Figure 5: Parameterization of manifold $Z_c$

The parameterization of the implicitly defined manifold $Z_c$ was another problem that had to be tackled. Due to the position, shape and temporal evolution of $Z_c$ we chose a parameterization with polar coordinates which is then used for the mesh representation of $Z_c$ and texture mapping. The ranges of the state variables are given as $0 < x < x_{max}$, $0 < y < y_{max}$, and $0 < z < 1$. An arbitrary point Q on $Z_c$ is assigned two parameters $(\alpha,h)$ which are defined with respect to the reference point $P(x_{max} / y_{max} / 0)$ (see Figure 5). Parameter $\alpha$ is an angle which results by projecting Q onto the xy-plane and connecting the projected point with reference point P. A regular quadrilateral mesh on $Z_c$ is generated by successively rotating a plane (running through P and being normal to the xy-plane) around P and iteratively calculating the intersection curve of this plane and the implicit surface $Z_c$. Such an intersection curve is subdivided into segments of equal length, and the endpoints of the segments are taken as meshpoints of the quadrilateral grid. Parameter h of point Q thus describes the relative length when moving from Q down to the beginning of the corresponding intersection curve. The parameterization was designed in such a way that in the specific case of manifold $Z_c$ each pair of $(\alpha,h)$ corresponds to a unique point of $Z_c$.

### 3.3 Particle Systems

As described in section 2.2 the dynamics of the Wonderland system can be split into a slow motion in *x, y* and *p* with an almost constant *z* (reduced system), and a very fast motion of *z* with respect to the velocity of *x, y* and *p* (layer system). The flow close to the equilibrium manifolds is determined by the reduced system, whereas the flow farther away from these manifolds is determined by the layer system.
To make this effect visible, we display the dynamical system at one specific point in time and introduce a set of particles into the system. At a specific point in time the state variable *p* is fixed and therefore the manifold $Z_c$ also does not change. As we were especially interested in the reduced system, we positioned the particle origins on the curved manifold $Z_c$. Starting with an even distribution of particles on $Z_c$ and exposing the particles to the instantaneous flow of the system gives an impression of the underlying dynamics. Generating an even distribution of particles on the manifold has to take into account that the quadrilaterals of the mesh surface do not have the same size. Larger quadrilaterals have to be selected more often for particle placement. Each quadrilateral of the mesh structure is assigned an interval whose length corresponds to the area of the quadrilateral. The intervals are consecutively positioned on the real line. This gives a combined interval which corresponds to the area of the entire mesh. Selecting positions within this combined interval by a random number generator with even distribution assures that quadrilaterals are chosen with a frequency equal to their relative area.
The motion and velocity of the particles show very clearly the dynamics of the layer and the reduced system. Plate 7 is a snapshot of an animation sequence with particles. As long as the particles remain close to the manifolds, their motion is determined by the reduced system. Thus these particles move rather slowly. When a particle leaves the neighborhood of an equilibrium manifold, its motion becomes more and more influenced by the layer problem, leading to a much faster motion of these particles. The equilibrium manifolds are no streamsurfaces. Therefore particles cross the manifold $Z_c$ with the flow being parallel to the xy-plane at the crossing points. Particles reaching the

border of phase space are eliminated and instead new particles are generated, again evenly distributed on $Z_c$.

It has to be pointed out that the particle system does not show an actual flow within the Wonderland model, but only the instantaneous flow for an infinitesimal small time period. This avoids that the particle motion and the motion of the manifold $Z_c$ are superimposed which makes interpretation more difficult. The instantaneous flow is well suited to give an insight into the dynamics of the reduced and layer system.

### *3.4 Tufts*

In this section an approach is discussed to visualize the flow close to the equilibrium manifold $Z_c$ during its temporal evolution. Over time the state variable *p* changes thus producing a manifold $Z_c$ with changing shape and position in phase space.

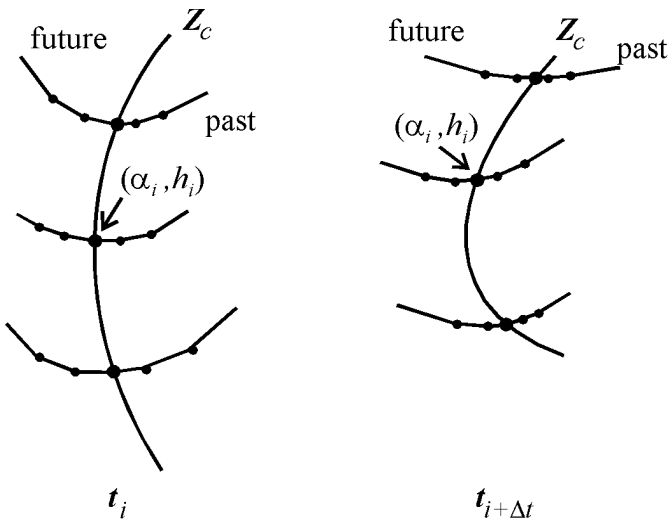


Figure 6: Tufts with constant temporal length fixed at the changing manifold $Z_c$

The flow in the vicinity of the moving manifold $Z_c$ is illustrated by using a tuft-like technique, i.e., objects displayed are short tubes that evolve like trajectories according to the underlying dynamics. Specific positions $(\alpha_i, h_i)$ on the manifold are selected and from these positions the flow is calculated in forward and backward direction for a short but constant period of time (see Figure 6). Forward integration visualizes the future and backward integration the past flow near manifold $Z_c$. As in each time step points $(\alpha_i, h_i)$ change position the forward and backward integration has to be done repeatedly. The tufts are represented as cylindrical tubes with transparency increasing as one moves from the starting position on the manifold to the loose end. The tufts have the same temporal length but due to the slow-fast dynamics of the Wonderland model the spatial length may vary considerably. Depending on the stability property of an initial position $(\alpha_i, h_i)$ (repelling or attracting) the forward or backward branch of a tuft may collapse to a single point or may remain within manifold $Z_c$. For an example see color plate 8. The distinction between the forward part and the backward part of a tuft is again done with color coding.

## 4. Implementation and Results

Visualization experiments on the Wonderland model have been done with AVS [AVS92] on an SGI graphics work station. The data-flow model of AVS and easy handling of user written modules makes AVS a suitable tool for testing and adapting our various visualization approaches.

In addition to modules supported by AVS we implemented a module *'Wonderland'*, which numerically simulates the various components of the Wonderland model. The outports of the *'Wonderland'* module provide trajectories and tufts as one-dimensional polylines. Connecting these ports to the AVS supported module *'Tube'* generates cylindrical three-dimensional representations which are then displayed with the module *'geometry viewer'*. Furthermore the *'Wonderland'* module calculates the equilibrium manifolds as quadrilateral meshes with corresponding texture coordinates. The borders of the manifolds are again given as polylines. Another output port of *'Wonderland'* is responsible for the particle system of the instantaneous flow. In this case particles are generated for efficiency reasons as small little triangles. The *'Wonderland'* module allows the user to interactively modify many simulation parameters, e.g., system parameters, starting position and length of trajectories, number of particles, number and position of tufts and others. Therefore parameter fine tuning and experimental adaptation of visualization techniques becomes quite easy.

After testing the chosen visualization approaches with AVS, we transferred the methods to Autodesk's '3D Studio' [Stud94], a high-end rendering software system, which includes an interface to user implemented software components. Since '3D Studio' is designed for animation artists, effects like camera animation and animated textures can be defined rather easily. Therefore this rendering software was used for the production of the final images and animation sequences, whereas AVS has been employed in the development and adaptation of the visualization methods. Post

production with 3D Studio is much more time consuming in comparison to the short turn-around cycles by using AVS during the development phase. But the produced images are much more sophisticated as the full rendering capabilities of '3D studio' are applicable.
In addition to the color plates various animation sequences were produced to illustrate the techniques described in this work. There is a sequence which shows trajectories of the dream, horror and escape scenario simultaneously. Other sequences show the temporal evolution of each of the scenarios together with the development of the corresponding equilibrium manifolds. Finally there are animation sequences illustrating the instantaneous flow with particle systems and the flow close to the manifolds with tufts. The color plates and the animation sequences are available at `http://www.cg.tuwien.ac.at/~rainer/vis96/`.

## 5. Conclusion

This work describes the investigation and visualization of a special class of analytically defined dynamical systems. The Wonderland model is an econometric model which describes interactions between population size, economic activity and environmental pollution. It is characterized by a pronounced slow-fast dynamics, i.e., certain state variables change much faster than others. Furthermore the topological structure of the system is determined by equilibrium manifolds which are not streamsurfaces and which are therefore crossed by the system flow.
Various visualization techniques are applied and adapted to the Wonderland model. These include velocity visualization with animated textures, visualizing equilibrium manifolds, and illustration of the local flow close to manifolds with particle systems and tufts. Adaptation of advanced visualization techniques to the specific needs of complex dynamical systems like the Wonderland model facilitates a better understanding of the underlying dynamics. Although econometrics scientists have been working on the Wonderland model for quite a while, some aspects of the model behavior (e.g., specific folding of manifold $Z_c$) were fully recognized in their implications only through the application of advanced visualization techniques.

## 6. Acknowledgments

The authors would like to thank Alexandra Milik, Alexia Prskawetz, Gustav Feichtinger (Institute for Econometrics, Operations Research and Systems Theory, Technical University Vienna), and Warren C. Sanderson (Department of Economics, State University of New York, Stony Brook) for providing us with the Wonderland model and for fruitful discussion during the visualization project.

## 7. References

[AVS92] *'AVS User's Guide'*, Advanced Visual Systems Inc., (1992)

[CaLe93] **B. Cabral, L.C. Leedom**, 'Imaging Vector Fields Using Line Integral Convolution', Proceedings SIGGRAPH '93.

[Feni79] **N. Fenichel,** *'Geometric Singular Perturbation Theory'*, Journal of Differential Equations, Vol. 31, pp. 53-98, (1979).

[GrWe95] **E. Gröller, R. Wegenkittl, A. Milik, A. Prskawetz, G. Feichtinger, W. C. Sanderson,** *'The Geometry of Wonderland',* to be published in *'Chaos, Solitons & Fractals'*, (1996).

[Hans93] **Ch. Hansen,** 'Visualization of Vector fields (2D and 3D)', SIGGRAPH 93, Course notes no 2., Introduction to Scientific Visualization, Tools and Techniques, 1993

[Jone95] **C. Jones,** *'Geometric Singular Perturbation Theory'*, in *'Dynamical Systems'*, Springer Lecture Notes Math., Vol. 1609, pp. 44-120, (1995).

[MiPr95] **A. Milik, A. Prskawetz, G. Feichtinger, W. C. Sanderson,** *'Slow-Fast Dynamics in Wonderland'*, Technical Report no. 177, Institute for Econometrics, Operations Research and Systems Theory, Technical University of Vienna, (1995).

[MiRo80] **E. F. Mishchenko, N. K. Roszow,** *'Differential Equations with Small Parameters and Relaxation Oscillations'*, Plenum Press, New York and London, (1980).

[PoWa93] **F.H. Post, T. van Walsum,** 'Fluid Flow Visualization' in H. Hagen, H. Müller, G.M. Nielson (eds.), Focus on Scientific Visualization, 1993, Springer, pp. 1-40.

[PoWi94] **F.H. Post, J.J. Wijk,** 'Visual Representation of Vector Fields: Recent Developments and Research Directions' in Rosenblum et al. (eds.), Scientific Visualization - Advances and Challenges, 1994, Academic Press, pp. 367-390.

[Sand94] **W. C. Sanderson,** *'Population - Development - Environment. Understanding their Interactions in Mauritius'*, in: **W. Lutz,** *'Simulation Models of Demographic, Economic, and Environmental Interactions'*, pp. 33-71, Springer, Berlin, (1994).

[Stud94] *'3D Studio V. 4.0'*, Autodesk Inc. (1994)

[Tson92] **A.A. Tsonis,** *'Chaos : From Theory to Applications'*, Plenum Press, (1992).

[Wijk91] **J.J. van Wijk**, Spot Noise, Proceedings SIGGRAPH '91, July 1991, pp. 309-318.